



Article

Experimental Study on the Cross-Scale Relationship of Cemented Backfill under the Action of an Air-Entraining Agent

Xiaosheng Liu ¹, Dongjie Yang ^{2,*} and Weijun Wang ¹

¹ School of Resources, Environment and Safety Engineering, Hunan University of Science and Technology, Xiangtan 411201, China; 1010109@hnust.edu.cn (X.L.); 1010038@hnust.edu.cn (W.W.)

² College of Safety Science and Engineering, Henan Polytechnic University, Jiaozuo 454003, China

* Correspondence: ydj@hpu.edu.cn

Abstract: Air-entraining agents have the function of optimizing pores and improving the performance of backfill. In this study, we used tailings and cement as the main raw materials and added different amounts of air-entraining agents to make backfill samples. By testing the uniaxial compressive strength (UCS) and microstructure, macro- and micro characteristics were studied. Nuclear magnetic resonance technology was used to explore pore characteristics, and fractal theory was used to quantitatively discuss the complexity of pore structure. Finally, a cross-scale relationship model between UCS and pores was established. The main conclusions are as follows: (1) Adding the appropriate amount of air-entraining agents can optimize pore structure and increase the UCS of backfill materials, which is beneficial to backfill materials. (2) The pores of backfill materials have fractal characteristics, the fractal effects of pores with different pore size ranges are different, and the air-entraining agent has a certain influence on the fractal characteristics of the pores. (3) There are inverse relationships between UCS and different pore size ranges.

Keywords: cemented backfill; air-entraining agent; macroscopic and microscopic characteristics; fractal theory; cross-scale relationship model



Citation: Liu, X.; Yang, D.; Wang, W. Experimental Study on the Cross-Scale Relationship of Cemented Backfill under the Action of an Air-Entraining Agent. *Fractal Fract.* **2023**, *7*, 821. <https://doi.org/10.3390/fractalfract7110821>

Academic Editors: Mei Yin, Mengxi Zhang, Yi Rui and Francesco Marotti De Sciarra

Received: 14 September 2023
Revised: 4 November 2023
Accepted: 9 November 2023
Published: 15 November 2023



Copyright: © 2023 by the authors. Licensee MDPI, Basel, Switzerland. This article is an open access article distributed under the terms and conditions of the Creative Commons Attribution (CC BY) license (<https://creativecommons.org/licenses/by/4.0/>).

1. Introduction

Backfill materials are filled into goaf, which can not only avoid surface subsidence, but also improve the safety of mining; as the source of backfill materials is solid waste, this can also reduce environmental pollution. Therefore, backfill materials can not only solve the problem of mine safety but also solve the problem of environmental pollution [1–3]. However, mines also have certain requirements for backfill materials, with the basic requirement being to achieve a certain level of fluidity and strength [4,5]. Adding an air-entraining agent (AEA) can improve the flowability of the filling slurry, but it also has a certain impact on the strength [6,7]. The AEA mainly changes the pore structure of the backfill material, and it also has a certain impact on the hydration reactions, thereby affecting the strength. At present, there are corresponding testing methods for studying pore characteristics and hydration products, mainly including mercury intrusion technology, nuclear magnetic resonance (NMR) technology, and scanning electron microscopy (SEM) technology [8–10].

NMR technology is a non-destructive testing technique that does not require the destruction of the sample to ensure its original morphology. It is mainly used to test pore characteristics and obtain the pore size distribution and content of backfill materials [11,12]. Jianhua Hu et al. used NMR technology to test the pore size distribution and content of backfill materials under different curing humidity levels [12]. SEM is a technique that uses magnification to observe the internal structure of backfill materials. When magnification is low, the distribution of pores and particles can be observed; in contrast, when magnification is high, hydration products and pore shapes can be observed [13,14]. Jiaxu Jin et al. used SEM technology to analyze the hydration products of backfill materials at high

magnification and the micro-cracks and pores of backfill materials at low magnification [13]. Further analysis of test data can provide more information. For SEM image treatment, the product category is generally judged according to the morphology of the hydration product, so it can only be qualitatively analyzed. For NMR data processing, some scholars have introduced fractal theory and used it to study the complexity of pores, thereby carrying out quantitative analysis [15–17]. Kang Zhao et al. studied the pore fractal characteristics of backfill materials with different cement–tailing ratios and different fiber types, eventually determining the influence relationship between various factors and pores [16]. According to different classification standards, pores can be classified into different categories. Depending on different peaks, they can be divided into large and small pores, and according to the degree of damage, they can be divided into harmful and harmless pores [11,15,18]. The fractal results vary depending on the type of pore.

Based on the above research foundation and shortcomings, this study uses tailings and cement as raw materials and adds different amounts of air-entraining agents to create backfill materials. Their macroscopic and microscopic characteristics are tested using a uniaxial compression test, NMR, and SEM, and fractal theory is used to analyze pore characteristics; finally, a cross-scale relationship between strength and pore characteristics is established. Thus, the macroscopic and microscopic characteristics of backfill materials and their relationships are studied under the action of air-entraining agents.

2. Experimental Preparation

2.1. Raw Materials

The tailings used in the experiment were graded tailings, and their particle size distribution is shown in Figure 1 after testing with a laser particle size analyzer. The physical properties of graded tailings were tested according to the GB/T 14684-2011 standard [19], and the results are shown in Table 1. The cement used was a composite Portland cement produced in Changsha. The experimental water used was daily drinking water in Changsha, and the AEA used was a commercially available product, with the main component being K12.

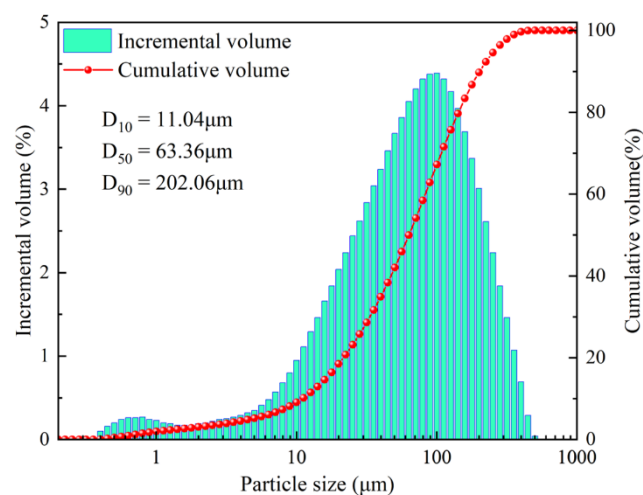


Figure 1. Particle size distribution of tailings.

Table 1. Physical properties of graded tailings.

Sample	Packing Density/(t/m ³)	Maximum Porosity/%	Natural Repose Angle/°
Graded tailings	1.57	49.5	37.5

2.2. Experimental Scheme

The slurry concentration used in this experiment was 70%, the cement/sand ratio was 1:8, and the additive was an air-entraining agent. The cement addition amounts were 0%, 0.2%, 0.4%, 0.6%, and 0.8%, respectively, denoted as A0, A1, A2, A3, and A4. There were 6 samples in each group and a total of 30 samples, among which 3 samples were used for strength testing and 3 samples were used for NMR testing. The samples used for SEM were taken from the damaged fragments after strength testing. The sample preparation and testing methods were as follows: The filling slurry was prepared according to the ratio and then injected into the standard mold (50 × 100 mm); after demolding, it was placed in a curing box for 14 days, and finally, various tests were conducted. The strength test was conducted using the WHY-300/10 pressure testing machine produced by Shanghai Hualong Testing Instrument Co., Ltd. The testing loading rate was 0.2 kN/s, and the sample was placed at the center of the loading plate. After the samples were tested, the fragments were selected from the center of the damaged samples, dried, sprayed with gold, and finally observed via SEM. The testing process of NMR was to first saturate the sample with water, wrap it with cling film, and finally use an NMR instrument for testing.

3. Testing Result Analysis

3.1. Strength

The strength characteristics of the backfill under the action of the AEA are shown in Figure 2. It can be observed in Figure 2 that the strength increases after adding AEA, but the excessive addition of AEA is harmful to the strength of the backfill, which illustrates that adding an appropriate amount of AEA has the effect of optimizing the pores of the backfill. This is because adding an appropriate amount of AEA in the same volume can introduce a small number of tiny bubbles, forming harmless pores, but when the content of AEA is too high, resulting in a large increase in the number of bubbles, the large number of bubbles gathered together will lead to an increase in the volume of the bubbles, resulting in the formation of harmful pores and reducing the strength. In the application process, the amount of AEA used was not too high so as to demonstrate its positive effect.

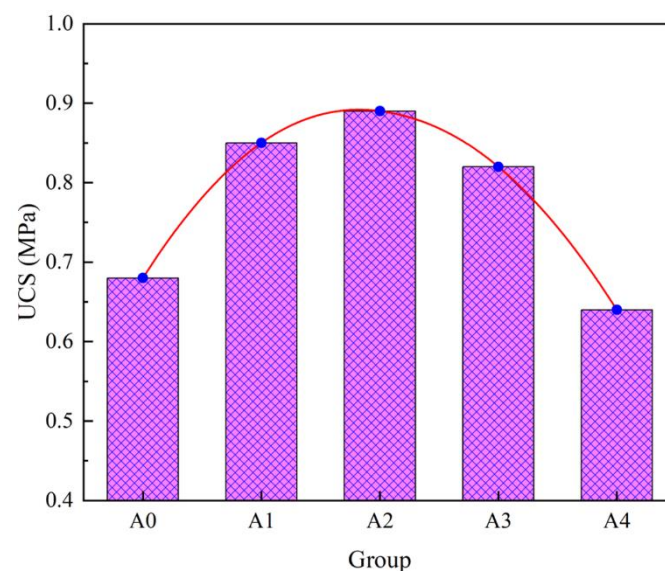


Figure 2. The strength characteristics of backfill materials.

3.2. NMR Characteristics

Pore characteristics are important parameters of backfill materials. According to relevant studies [11,15], pores can be divided into four categories according to pore size: harmless pores (<20 nm), less harmful pores (20~100 nm), harmful pores (100~200 nm), and multi-harmful pores (>200 nm). NMR can non-destructively test pore characteristics,

and the results are shown in Figure 3. According to relevant research [20,21], there is a certain relationship between pore size and T_2 value. Therefore, the T_2 value can reflect the distribution of pore size, and the relationship between them can be expressed as follows:

$$r \approx T_2 \rho_2 F_s = 36T_2 \quad (1)$$

where r represents the pore size (nm), T_2 represents the transverse relaxation time (ms), ρ_2 represents the transverse surface relaxation intensity (taken as 12 nm/ms), and F_s represents the pore shape factor (considered spherical, taken as 3) [22,23].

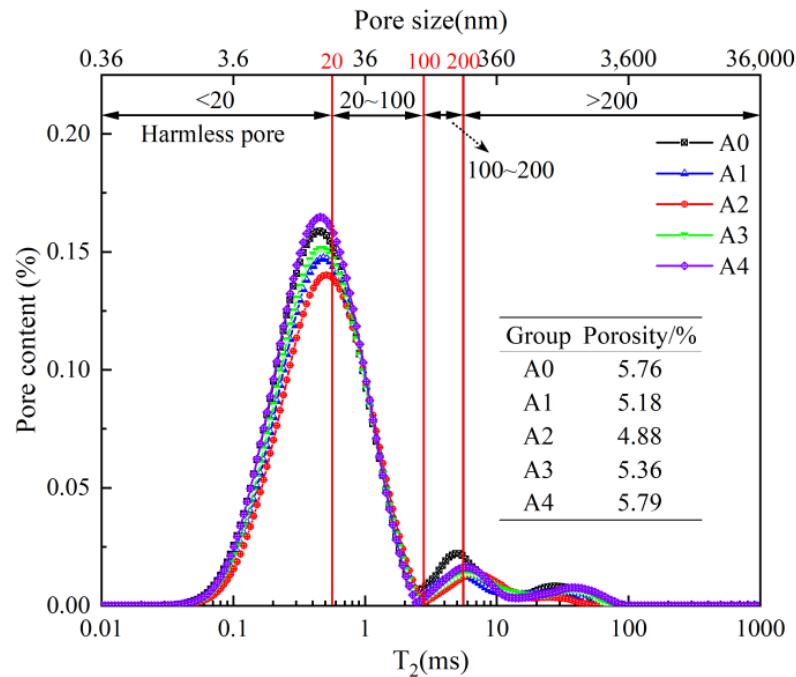


Figure 3. The T_2 spectrum of backfill materials.

It can be observed in Figure 3 that there are three peaks in the T_2 spectrum, indicating that the pores in the backfill can be divided into three categories, which are small, medium, and large pores. The larger the peak area, the greater the pore content, so most of the pores in the backfill are small pores. Some pores in small pores are harmless, while others are less harmful. As the content of AEA increases, the porosity shows a first decreasing and then increasing trend, which indicates that an appropriate amount of AEA has the effect of optimizing pores and reducing pore volumes.

3.3. Microstructure

SEM technology can magnify the substance thousands of times to observe the microstructure characteristics of the substance, but the SEM image can only qualitatively analyze the apparent characteristics of the substance. Figure 4 shows a SEM image of the backfill material magnified by 5000 times. From the SEM image, it can be seen that the hydration products are mainly acicular crystals (AFt) and flocculent (C-S-H), and the pores are filled with hydration products in a staggered manner. The smaller the pore size, the easier it is to fill, and the denser the backfill material. Conversely, the looser the backfill material, the lower its strength. The macroscopic changes in backfill materials can also be qualitatively explained via microscopic characteristics.

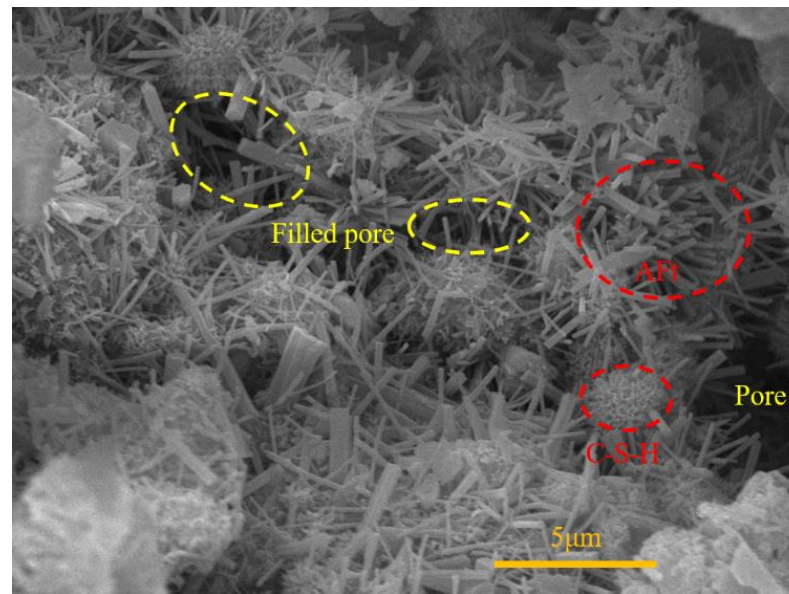


Figure 4. The SEM image of backfill materials magnified 5000 times.

4. Discussion

4.1. Fractal Characteristics

Pores are complex structures, and in order to characterize their complexity, fractal theory has been introduced in relevant studies [15,17,24,25]. Research has shown that there is a certain functional relationship between the pore's size and its volume content, and there is also a certain functional relationship between T_2 value and pore size, so they can be transformed. The relationship between pore size and volume is as follows:

$$S_v = \frac{r^{3-D}}{r_{max}^{3-D}} \quad (2)$$

where S_v represents the cumulative pore volume, r represents the pore size, r_{max} represents the max pore size, and D represents the fractal dimension of pores. We substitute Equation (1) into Equation (2) to obtain the relationship between T_2 value and volume:

$$S_v = \frac{T_2^{3-D}}{T_{2max}^{3-D}} \quad (3)$$

where T_{2max} represents the max transverse relaxation time. The functional relationship of the fractal dimension is obtained by taking the logarithm of both sides of Equation (3):

$$\lg(S_v) = (3 - D)\lg(T_2) + (D - 3)\lg(T_{2max}) \quad (4)$$

The fractal dimension of the pore can be obtained via the linear fitting of $\lg(S_v)$ and $\lg(T_2)$. Taking group A0 as an example that needs solving, the results are shown in Figure 5. From Figure 5, it can be seen that the fitting effect of pores within each range of pore size is good, and the larger the pore size, the greater the fractal dimension. When the pore size range increases for fitting, the fitting effect deteriorates because the pore size spacing is large, which weakens the similarity between larger and smaller pore sizes.

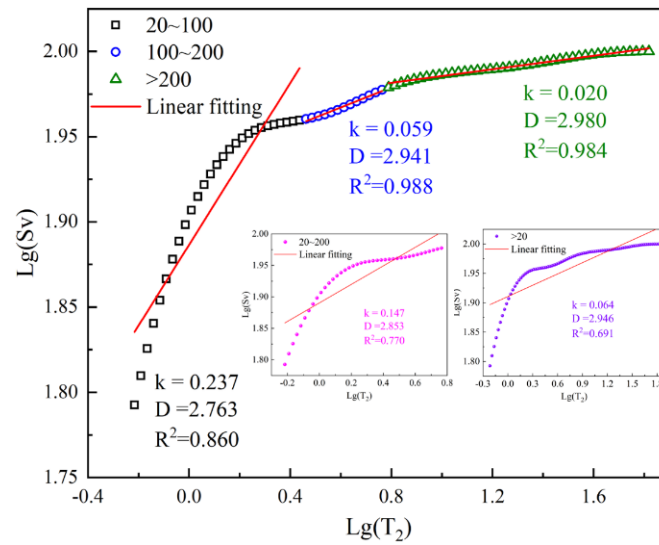


Figure 5. The fractal dimension of pores within each range of pore size (group A0).

Each group is calculated according to the above calculation methods, and the results are shown in Table 2. From the table, it can be seen that the fractal dimensions of pores within some ranges of pore sizes have a certain regularity. For example, the fractal dimensions of pores within the range of 20~100 nm show a first decreasing and then increasing trend with respect to the groups, and the fitting effect within this range is good. The fractal dimensions of some pores also have no regularity; for example, pores within the range of >200 nm have no regularity. This also indicates that the air-entraining agent mainly acts on small pores.

Table 2. The fractal dimensions of all groups’ backfill.

Group	D			R ²						
	20–100	100–200	>200	20–200	>20	>200	20–200	>20		
A0	2.763	2.941	2.980	2.853	2.946	0.860	0.988	0.984	0.770	0.691
A1	2.733	2.960	2.982	2.839	2.935	0.868	0.993	0.985	0.752	0.629
A2	2.707	2.971	2.982	2.828	2.929	0.876	0.960	0.888	0.739	0.620
A3	2.747	2.967	2.981	2.848	2.941	0.862	0.977	0.977	0.733	0.636
A4	2.765	2.962	2.983	2.861	2.948	0.849	0.978	0.980	0.726	0.633

4.2. The Relationship between Strength and Pores

The pore content in the backfill material has a certain influence on strength, but the influence does not exhibit the following: the higher the pore content, the lower the strength. Only when the harmful pores in the backfill material increase do they have a certain impact on strength. The relationship between pore content and strength was established, and the results are shown in Figure 6. It can be observed in Figure 6 that both porosity and harmful pore content increase, leading to a decrease in strength. The relationships between them are as follows:

$$\begin{aligned}
 y &= -0.272x + 2.245 \\
 y &= -1.366x + 3.827
 \end{aligned}
 \tag{5}$$

where x represents pore content (%), and y represents strength (MPa). It can be observed in Formula (5) that the strength decreases linearly with the pore content. Therefore, reducing the porosity and reducing the harmful pore content are effective methods for improving strength. Adding an appropriate amount of AEA can not only reduce porosity but also optimize the pore structure, which has an improved effect on strength. However, adding

too much AEA should be avoided; otherwise, it will increase harmful pore contents and reduce the strength of the backfill.

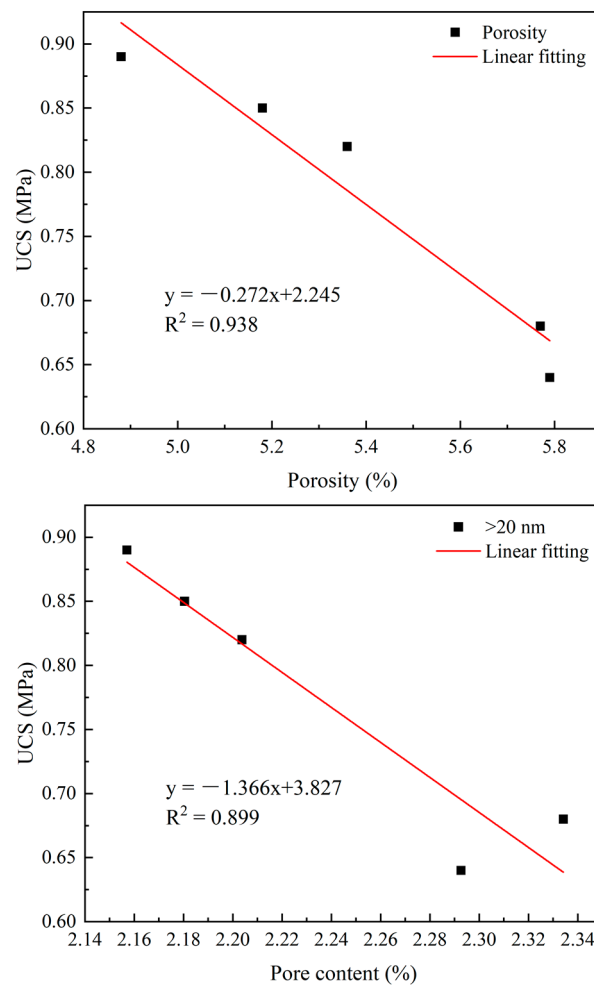


Figure 6. The relationship between pores and strength.

4.3. The Relationship between Strength and Fractal Dimension

The fractal dimension reflects the complexity of pores, and pores have a certain impact on strength, so there is a certain functional relationship between fractal dimensions and strength. Figure 7 shows the functional relationship between strength and fractal dimensions. It can be observed in the figure that strength decreases as the fractal dimension increases, which is consistent with the research results of other scholars [15,17]. Their relationships are as follows:

$$y = -0.007e^{(66.667 \times (x - 2.711))} + 0.890 \quad (6)$$

$$y = -7.981x + 23.488 \quad (7)$$

$$y = -13.144x + 39.417 \quad (8)$$

where x represents the fractal dimension, and y represents strength (MPa). It can be observed in the formulas that the relationships differ within the different pore size ranges. There is an exponential decreasing relationship between them within the range of 20~100 nm and a linear decreasing relationship between them within the range of 20~200 nm and >20 nm. This also indicates that different pore sizes have different effects on strength, and as the pore size range increases, the effect of fractal dimensions on strength tends to become

simplified. The comparative analysis indirectly reflects that the AEA has a significant impact on small pores.

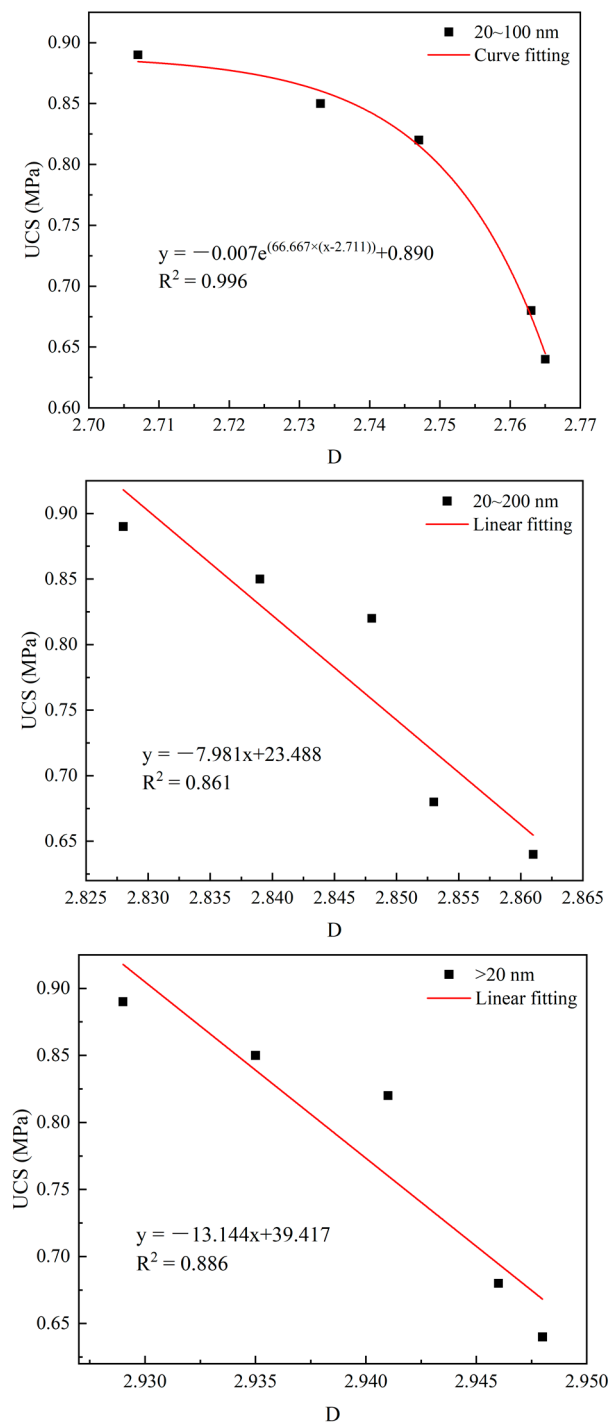


Figure 7. The relationship between fractal dimensions and strength.

5. Conclusions

The addition of AEA has a certain impact on the performance of backfill materials. This study utilized a uniaxial compression test, NMR, and SEM to study the macroscopic and microscopic characteristics of backfill materials. Fractal theory was used to analyze the complexity of the pore structure, and a cross-scale relationship model was established. The main conclusions are as follows:

- (1) AEA has the effect of optimizing the pore's structure. Adding an appropriate amount of AEA can reduce pore contents and increase the strength of the backfill material, which is beneficial for the backfill material.
- (2) The fractal effects of pores differ with different pore size ranges. Via fractal analyses of pores within different pore size ranges, it was found that the fractal effects of pores within different pore size ranges are different. The fractal effects of pores within 100~200 nm and >200 nm ranges were best.
- (3) A cross-scale relationship model was established. By establishing the relationship between strength and pore characteristics, it was found that strength has an inversely proportional relationship to the pore content and fractal dimension of pores within different pore size ranges.
- (4) The pore's morphology characteristics require further analysis. The meaning of the fractal dimension in relation to the morphology of the pores requires other means for further study.

Author Contributions: Methodology, D.Y. and W.W.; Formal analysis, D.Y.; Writing—original draft, X.L.; Writing—review & editing, X.L.; Funding acquisition, X.L. and W.W. All authors have read and agreed to the published version of the manuscript.

Funding: This study was supported by the Hunan Provincial Natural Science Foundation (Grant no. 2023JJ50356) and the National Natural Science Foundation of China (Grant no. 52074115).

Data Availability Statement: No new data were created or analyzed in this study. Data sharing is not applicable to this article.

Conflicts of Interest: The authors declare no conflict of interest.

References

1. Zhou, Y.W.; Zhang, T.; Duan, L.C.; Li, J.W. Summary of research on comprehensive treatment of mine goaf in china. *Saf. Environ. Eng.* **2022**, *29*, 220–230.
2. Wu, J.H. Development Status and Prospect of Filling Mining Technology in China. *Shanxi Coking Coal Sci. Technol.* **2022**, *46*, 7–11.
3. Liu, L.; Fang, Z.Y.; Zhang, B.; Wang, M.; Qiu, H.; Zhang, X. Development history and basic categories of mine backfill technology. *Met. Mine* **2021**, *3*, 1–10.
4. Liu, G.; Li, L.; Yao, M.; Landry, D.; Malek, F.; Yang, X.; Guo, L. An Investigation of the Uniaxial Compressive Strength of a Cemented ydraulic Backfill Made of Alluvial Sand. *Minerals* **2017**, *7*, 4. [[CrossRef](#)]
5. Zhao, F.; Hu, J.; Liu, T.; Zhou, T.; Ren, Q. Study of the Macro and Micro Characteristics of and Their Relationships in Cemented Backfill Based on SEM. *Materials* **2023**, *16*, 4772. [[CrossRef](#)]
6. Yang, B.; Wang, X.; Yin, P.; Gu, C.; Yin, X.; Yang, F.; Li, T. The Rheological Properties and Strength Characteristics of Cemented Paste Backfill with Air-Entraining Agent. *Minerals* **2022**, *12*, 1457. [[CrossRef](#)]
7. Hu, J.H.; Kuang, Y.; Zhou, T.; Zhao, F.W. Influence of Air Entraining Agent on Strength and Microstructure Properties of Cemented Paste Backfill. *IEEE Access* **2019**, *7*, 140899–140907. [[CrossRef](#)]
8. Yao, Y.B.; Liu, D.M. Comparison of low-field NMR and mercury intrusion porosimetry in characterizing pore size distributions of coals. *Fuel* **2012**, *95*, 152–158. [[CrossRef](#)]
9. Zhu, Z.; Huo, W.; Sun, H.; Ma, B.; Yang, L. Correlations between unconfined compressive strength, sorptivity and pore structures for geopolymer based on SEM and MIP measurements. *J. Build. Eng.* **2023**, *67*, 106011. [[CrossRef](#)]
10. Rong, H.; Zhou, M.; Hou, H.B. Pore Structure Evolution and Its Effect on Strength Development of Sulfate-Containing Cemented Paste Backfill. *Minerals* **2017**, *7*, 8. [[CrossRef](#)]
11. Zhang, Y.Z.; Gan, D.Q.; Xue, Z.L.; Liu, Z.Y.; Chen, X. Correlation Mechanism Between Pore Structure and Backfill Strength Based on NMR Technology. *Adv. Eng. Sci.* **2022**, *54*, 121–128.
12. Hu, J.; Zhao, F.; Ren, Q.; Kuang, Y.; Zhou, T.; Luo, Z. Microscopic characterization and strength characteristics of cemented backfill under different humidity curing conditions. *R. Soc. Open Sci.* **2019**, *6*, 191227. [[CrossRef](#)] [[PubMed](#)]
13. Jin, J.X.; Qin, Z.F.; Zuo, S.H.; Feng, J.J.; Sun, Q. The Role of heological Additives on Fresh and Hardened Properties of Cemented Paste Backfill. *Materials* **2022**, *15*, 3006. [[CrossRef](#)] [[PubMed](#)]
14. Qiu, H.; Zhang, F.; Liu, L.; Huan, C.; Hou, D.; Kang, W. Experimental study on acoustic emission characteristics of cemented rock-tailings backfill. *Constr. Build. Mater.* **2022**, *315*, 125278. [[CrossRef](#)]
15. Liu, L.; Fang, Z.; Qi, C.; Zhang, B.; Guo, L.; Song, K.-I. Experimental investigation on the relationship between pore characteristics and unconfined compressive strength of cemented paste backfill. *Constr. Build. Mater.* **2018**, *179*, 254–264. [[CrossRef](#)]
16. Zhao, K.; Ma, C.; Yang, J.; Wu, J.; Yan, Y.; Lai, Y.; Ao, W.; Tian, Y. Pore fractal characteristics of fiber-reinforced backfill based on nuclear magnetic resonance. *Powder Technol.* **2023**, *426*, 118678. [[CrossRef](#)]

17. Zhao, F.; Hu, J.; Yang, Y.; Xiao, H.; Ma, F. Cross-Scale Study on Lime Modified Phosphogypsum Cemented Backfill by Fractal Theory. *Minerals* **2022**, *12*, 403. [[CrossRef](#)]
18. Zhang, M.; Zhang, P.; Zhang, H.B. Pore structure of concrete materials. *Sci. Technol. Inf.* **2007**, *36*, 139–140.
19. GB/T 14684-2011; Sand for Construction. Standardization Administration of the People's Republic of China: Beijing, China, 2011.
20. Li, J.L.; Kaunda, R.B.; Zhou, K.P. Experimental investigations on the effects of ambient freeze-thaw cycling on dynamic properties and rock pore structure deterioration of sandstone. *Cold Reg. Sci. Technol.* **2018**, *154*, 133–141. [[CrossRef](#)]
21. Deng, H.; Tian, G.; Yu, S.; Jiang, Z.; Zhong, Z.; Zhang, Y. Research on Strength Prediction Model of Sand-like Material Based on Nuclear Magnetic Resonance and Fractal Theory. *Appl. Sci.* **2020**, *10*, 6601. [[CrossRef](#)]
22. Gao, R.G.; Zhou, K.P.; Liu, W.; Ren, Q.F. Correlation between the Pore Structure and Water Retention of Cemented Paste Backfill Using Centrifugal and Nuclear Magnetic Resonance Methods. *Minerals* **2020**, *10*, 610. [[CrossRef](#)]
23. Li, J.L.; Liu, H.W.; Ai, K.M.; Zhu, L.Y. An NMR-Based Experimental Study on the Pore Structure of the Hydration Process of Mine Filling Slurry. *Adv. Civ. Eng.* **2018**, *2018*, 4720356. [[CrossRef](#)]
24. Hu, J.; Zhao, F.; Kuang, Y.; Yang, D.; Zheng, M.; Zhao, L. Microscopic characteristics of the action of an air entraining agent on cemented paste backfill pores. *Alex. Eng. J.* **2020**, *59*, 1583–1593. [[CrossRef](#)]
25. Liu, Y.; Deng, H.W. Study on permeability performance of cemented tailings backfill based on fractal characteristics of pore structure. *Constr. Build. Mater.* **2023**, *365*, 130035. [[CrossRef](#)]

Disclaimer/Publisher's Note: The statements, opinions and data contained in all publications are solely those of the individual author(s) and contributor(s) and not of MDPI and/or the editor(s). MDPI and/or the editor(s) disclaim responsibility for any injury to people or property resulting from any ideas, methods, instructions or products referred to in the content.